Testing the no-hair theorem with LIGO and Virgo

Maximiliano Isi [1]

e-mail: maxisi@mit.edu

LIGO Laboratory, Massachusetts Institute of Technology,
Cambridge, Massachusetts 02139, USA

Abstract

The no-hair theorem predicts that a perturbed Kerr black hole should emit gravitational waves as damped sinusoids with characteristic frequencies and damping rates depending only on the hole's mass and spin. Analyzing the spectrum of such quasinormal modes can provide a direct probe of the black-hole spacetime, distinguishing it from other compact objects and enabling tests of general relativity. Considering the two least-damped components of the dominant angular mode ($\ell = m = 2$, $n \leq 1$), we find that the first LIGO detection (GW150914) already encoded clues about the black-hole spectrum. A two-mode ringdown model allows us to measure the final mass and spin of the remnant exclusively from postinspiral data, obtaining an estimate in agreement with that from the full signal. We also find that an independent measurement of the frequency of the second mode yields agreement with the no-hair hypothesis at the $\sim 20\%$ level. Improved detectors on the ground, as well as future missions in space, will provide even stronger tests. *This is a summary of Isi, Giesler, Farr, Scheel, and Teukolsky (2020) [1].*

1 Introduction

The last portion of the gravitational waves (GWs) from a binary black hole (BH) coalescence corresponds to the ringdown of the remnant object. In general relativity (GR), this ringdown radiation takes the form of superposed damped sinusoids, corresponding to the quasinormal modes (QNMs) of the final Kerr BH [2, 3, 4, 5]. The frequencies and decay rates of these damped sinusoids are uniquely determined by the final hole's mass M_f and dimensionless spin magnitude χ_f. This follows from the *no-hair theorem*—the statement that mass and spin are the only two properties of astrophysical black holes in GR. Teasing out the QNMs from GW observations could allow us to test GR, and distinguish Kerr remnants from possible mimickers by testing the no-hair theorem [6, 7, 8, 9, 10, 11, 12, 13, 14].

In [1], we analyze LIGO [15] data from the GW150914 event [16] to perform a multimodal spectroscopic analysis of a BH ringdown. Following [17], we rely on tones of the $\ell = m = 2$ angular mode to measure M_f and χ_f from data starting at the peak of the signal, assuming first that QNMs are as predicted by perturbation theory for a Kerr BH. This measurement agrees with that from the longest-lived mode alone beginning $3 \, \text{ms}$ after the waveform peak amplitude [18], as well as that obtained from the full waveform using fits to numerical relativity. We also consider a two-tone model that allows deviations from the Kerr prediction for any given mass and spin. From data starting at
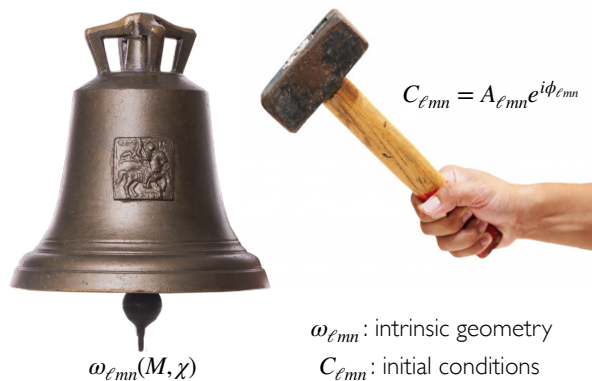
---

[1]NHFP Einstein fellow

Figure 1: A perturbed BH rings just like a struck bell. The frequency $\omega_{\ell mn}$ and damping rate (pitch and duration) encode information about the intrinsic geometry of the object: mass and spin for a Kerr BH, shape and material for a bell. The complex amplitudes $C_{\ell mn} = A_{\ell mn}e^{i\phi_{\ell mn}}$, on the other hand, carry information about the origin of the perturbation. (*Image source:* bell [33], hammer [34].)

peak strain, we find the spectrum to be in agreement with the no-hair hypothesis to within $\sim 20\%$, with 68% credibility. This is a test of the no-hair theorem based purely on the postinspiral regime.

Previous analyses had looked for the ringdown in data at late times after the signal peak, where the QNMs are too weak to confidently characterize with current instruments [19, 20, 21, 22, 23, 24, 25]. This was motivated by concerns about potential nonlinearities surrounding the BH merger [9, 26, 27, 21, 22, 24, 25]. However, the linear description can be extended to the full waveform following the peak of the gravitational wave strain: times around the peak are dominated by ringdown *overtones*— the QNMs with the fastest decay rates [17, 28]. Indications of this can be found in the waveform modeling literature, with overtones an integral part of early equivalent one-body models [29, 30, 31]. Yet, with a few exceptions [13, 23], previous ringdown analyses have neglected overtones [9, 19, 32, 20, 21, 22, 24, 25]. As a consequence, these studies ignored were unable to extract multiple ringdown modes.

The remaining sections of these Proceedings summarize the method and results of [1] as presented at the *3rd World Summit on Exploring the Dark Side of the Universe*, and conclude with a brief discussion on future perspectives.

2 Method

Each QNM has a frequency $\omega_{\ell mn}$ and a damping time $\tau_{\ell mn}$, where n is the overtone index and (ℓ, m) are indices of spin-weighted angular harmonics that describe the angular structure of the mode. The overtone index n orders the modes with a given (ℓ, m) by increasing damping rate, so that $n = 0$ denotes the longest-lived ("fundamental") mode. Unlike elsewhere in physics, a higher n does not imply a higher frequency ω_n; rather, the opposite is generally true.

Our analysis targets the fundamental and overtones of the $\ell = m = 2$ spin-weighted spherical harmonic of the strain, as this is the only angular harmonic expected to be relevant for GW150914 [35, 36, 25]. We drop the ℓ and m indices, and write the $\ell = m = 2$ mode of the ringdown strain ($h = h_+ - ih_\times$) as a sum of damped sinusoids [2, 3, 4, 5],

$$h_{22}^N(t) = \sum_{n=0}^{N} A_n \exp\left[-i\left(\omega_n t + \phi_n\right) - t/\tau_n\right], \tag{1}$$

for times t greater than some start time t_0, where $\Delta t = t - t_0$. N is the index of the highest overtone included in the model, which for us will always be $N \leq 2$. For a Kerr BH, all the ω_n's and
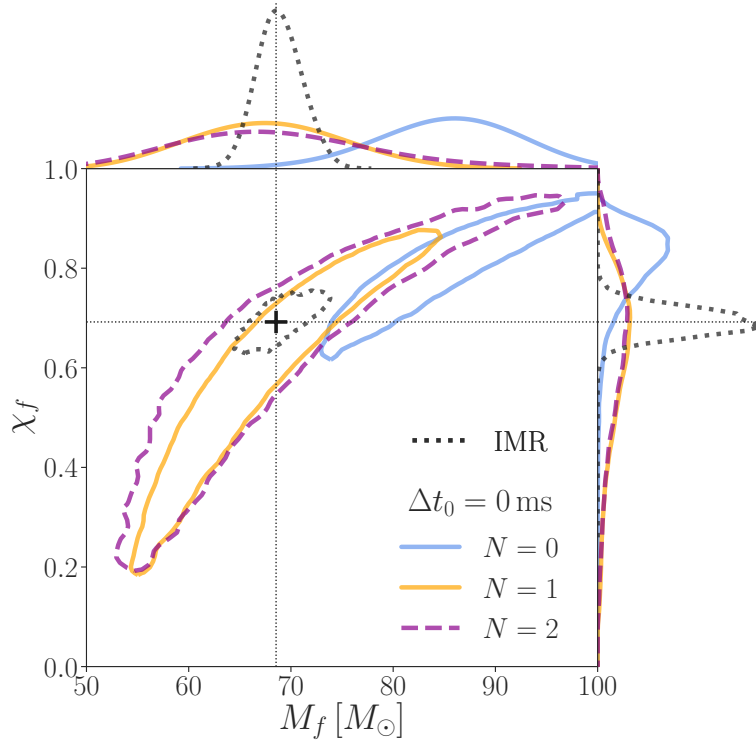
Figure 2: Contours represent 90%-credible regions on the remnant mass (M_f) and dimensionless spin magnitude (χ_f), obtained from the analysis of the GW150914 ringdown starting at peak strain amplitude ($\Delta t_0 = t_0 - t_{\text{peak}} = 0$). Color encodes the number of overtones N in the model: 0 (solid blue), 1 (solid yellow), 2 (dashed purple) The dotted black contour is obtained from the full IMR waveform, assuming GR; the crosshairs mark the peak of this distribution ($M_f = 68.5 M_\odot$, $\chi_f = 0.69$). The top and right panels show marginal posteriors for M_f and χ_f respectively. This is Fig. 1 in [1].

τ_n's are implicit functions of the remnant mass and spin magnitude (M_f, χ_f), and can be computed from perturbation theory [37, 38, 39]. The amplitudes A_n and phases ϕ_n cannot be computed within perturbation theory, so we treat them as free parameters (Fig. 1).

We carry out a Bayesian analysis of LIGO Hanford and LIGO Livingston data for GW150914 [16, 40, 41]. For a choice of N and start time t_0, we compute the joint posterior probability over M_f, χ_f, A_n and ϕ_n. We first do so assuming a Kerr spectrum, but then relax the $N = 1$ model to test the no-hair theorem: in this non-GR model, we write

$$\omega_1 = 2\pi f_1^{(\text{GR})} \left(1 + \delta f_1\right), \tag{2}$$

$$\tau_1 = \tau_1^{(\text{GR})} \left(1 + \delta\tau_1\right), \tag{3}$$

with δf_1 and $\delta\tau_1$ fractional deviations away from the Kerr values $f_1^{(\text{GR})}$ and $\tau_1^{(\text{GR})}$ for any given M_f and χ_f. In all cases, we parametrize start times via $\Delta t_0 = t_0 - t_{\text{peak}}$, where $t_{\text{peak}} = 1126259462.423$ GPS refers to the signal peak at the LIGO Hanford detector [42, 19]. We define the likelihood in the time domain in order to explicitly exclude all data before t_0. See the Supplement to [1] for details.

We compare our ringdown-only measurements to the expectation from the full inspiral-merger-ringdown (IMR) signal. We use fitting formulas based on numerical relativity [43, 44] to predict the remnant parameters from publicly-available posterior samples on the binary parameters [40, 45].
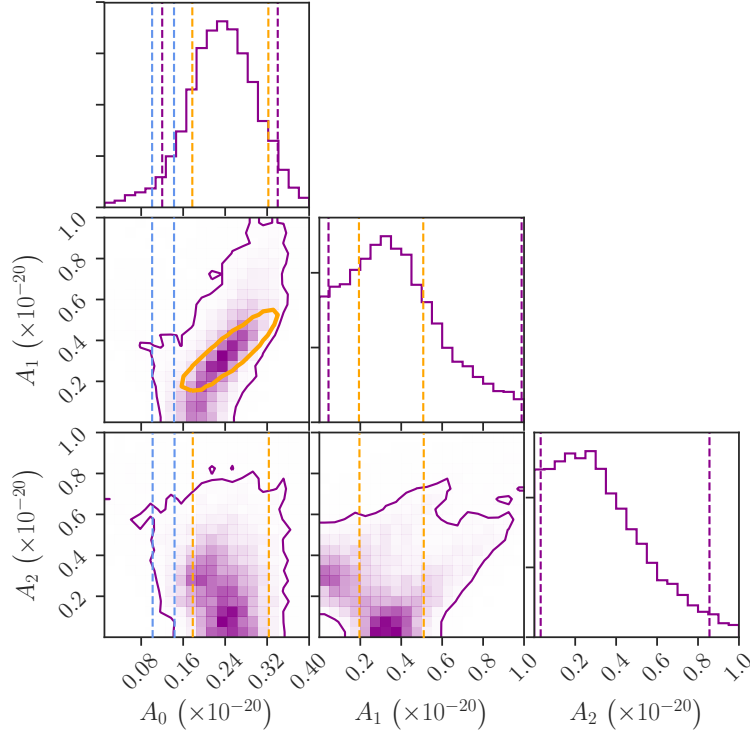
Figure 3: Measured QNM amplitudes for ringdown analyses with different number of overtones N, starting at peak strain: the joint posterior for A_0, A_1 and A_2 recovered by the $N = 2$ model (purple); the 90%-credible measurement of A_0 and A_1 obtained with $N = 1$ (yellow); and the same for A_0 obtained with $N = 0$ (blue). Solid curves and vertical dashed lines enclose 90% of the probability mass. Values have been rescaled by a constant to correspond to the strain measured by the LIGO Hanford detector. This is Fig. 2 in [1].

3   Results

Fig. 2 shows the 90%-credible regions for M_f and χ_f, obtained assuming a Kerr spectrum ($\delta f_n = \delta\tau_n = 0$) by analyzing data starting at t_{peak} with different numbers of overtones ($N = 0, 1, 2$) in the ringdown template of Eq. (1). Under GR, the ringdown and IMR measurements should agree. As expected for $\delta t_0 = 0$, this is only the case for the overtone results ($N \geq 1$), and not for the fundamental alone. Adding a second overtone ($N = 2$) does not improve agreement with IMR, which is expected given the network SNR of GW150914 [17].

The fact that the analysis is unable to unequivocally identify the second overtone in the data is reflected in the amplitude posteriors of Fig. 3. The $N = 2$ result supports a range of values for A_1 and A_2, but excludes $A_1 = A_2 = 0$ with 90% credibility (bottom center in Fig. 3). The joint posterior distribution on A_1 and A_2 tends to favor the first overtone at the expense of the second, favoring a value of A_1 in agreement with the $N = 1$ posterior (yellow traces in Fig. 3). Assuming $N = 1$, $A_1 = 0$ is disfavored at 3.6σ; assuming $N = 2$, $A_1 = A_2 = 0$ is disfavored with 90% credibility.

We next compare measurements carried out with overtones at the peak to those without overtones after the peak. Fig. 4 shows 90%-credible regions for the remnant mass and spin magnitude obtained with $N = 0$ at different times after t_{peak} ($\Delta t_0 \in [1, 3, 5]$ ms). As the overtones die out, the fundamental mode becomes a better model for the signal, and we find that the $N = 0$ contour coincides with the IMR measurement $\sim$3 ms after the peak, in agreement with [19].
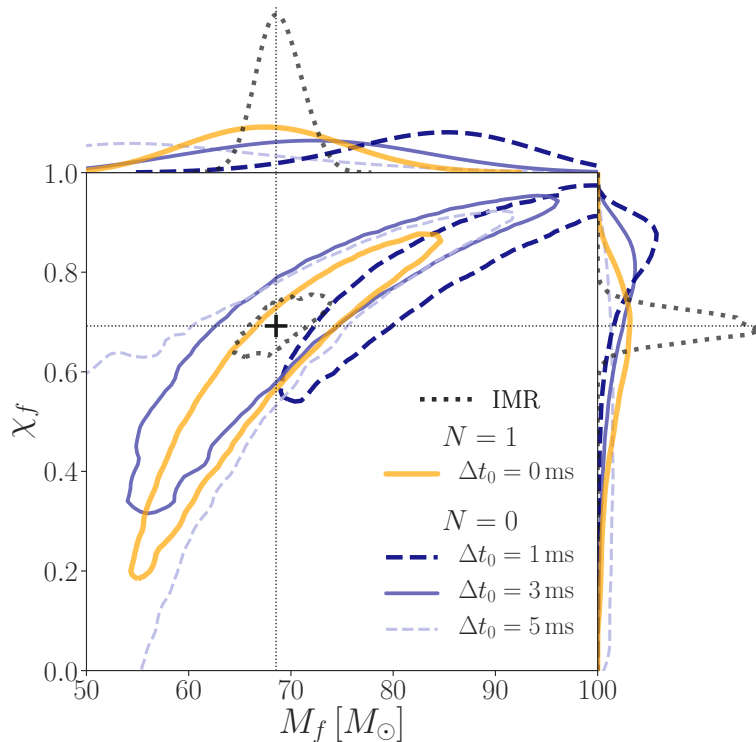
Figure 4: Contours represent 90%-credible regions on the remnant mass (M_f) and dimensionless spin magnitude (χ_f), obtained from the analysis of the GW150914 ringdown with $N = 0$ at different times after the peak (blue), compared to $N = 1$ at the peak. The dotted black contour is obtained from the full IMR waveform, assuming GR; the crosshairs mark the peak of this distribution ($M_f = 68.5 M_\odot$, $\chi_f = 0.69$). The top and right panels show marginal posteriors for M_f and χ_f respectively. Around $\Delta t_0 = 3\,\text{ms}$, the overtones have become unmeasurable and only the fundamental mode remains; consequently, at that time, the $N = 0$ result starts being consistent with both the full IMR waveform and the $N \geq 1$ models at the peak, in agreement with GR. This is Fig. 3 in [1].

Finally, we allow the first-overtone frequency and damping time to float around the no-hair values in the $N = 1$ model, starting the analysis at peak strain. Fig. 5 shows the resulting posterior over the δf_1 and $\delta \tau_1$. With 68% credibility, we measure $\delta f_1 = -0.05 \pm 0.2$, establishing agreement with the no-hair hypothesis ($\delta f_1 = 0$) at the 20% level. The damping time is largely unconstrained in the $-0.06 \lesssim \delta \tau_1 \lesssim 1$ range.

4   Conclusion

Making use of overtones, we extracted information about the GW150914 remnant using only postin-spiral data, starting at the peak of the signal (Fig. 2). We found evidence of the fundamental mode plus at least one overtone (Fig. 3), and measured the remnant mass and spin in agreement with that the full waveform analysis. This result is also consistent with the one obtained using solely the fundamental mode at a later time (Fig. 4).

The agreement between all measurements (IMR, $N = 0$, $N \geq 1$) is evidence that, beginning as early as the signal peak, a far-away observer cannot distinguish the source from a linearly perturbed Kerr background, i.e., we do not observe nonlinearities in this regime. The agreement between the IMR and postmerger estimates implies that the data conform to the full GR prediction, as in the IMR
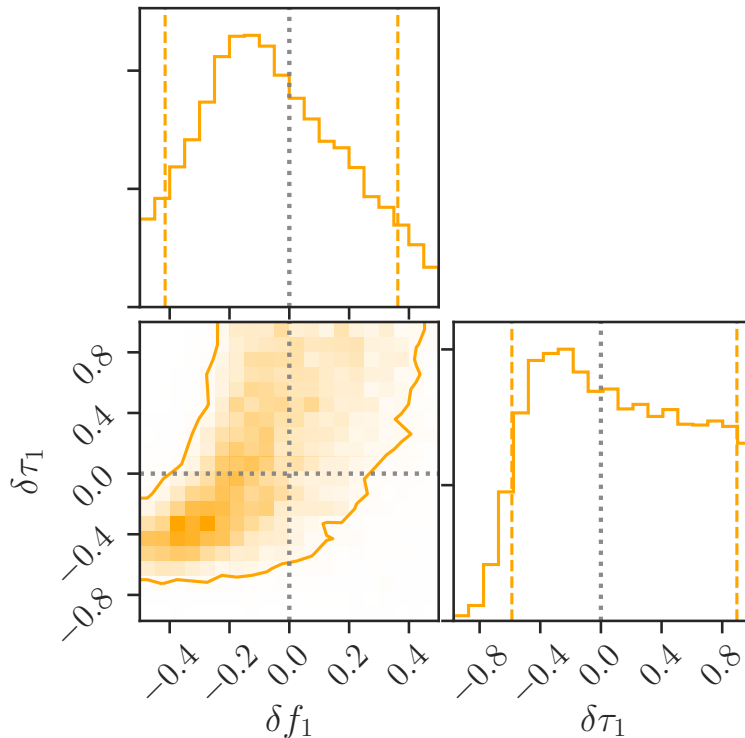
Figure 5: Posterior distribution of the fractional deviations δf_1 and $\delta \tau_1$ away from the no-hair value $\delta f_1 = \delta \tau_1 = 0$ (gray dotted lines), measured at peak strain with $N = 1$. The solid contour and dashed vertical lines enclose 90% of the posterior probability. Fixing $\delta f_1 = \delta \tau_1 = 0$ recovers the $N = 1$ analysis in Figs. 2 and 4. This is Fig. 4 in [1].

consistency test described in [46, 47].

With the identification of multiple ringdown modes, we took a step toward the goal of black hole spectroscopy. We constrained deviations away from the no-hair spectrum by allowing the overtone frequency and damping time to vary freely (Fig. 5). This is equivalent to independently measuring the frequencies of the fundamental and first overtone, and establishing their consistency with the Kerr hypothesis.

Future overtone measurements could potentially allow us to identify BH mimickers, and probe the applicability of the no-hair theorem with high precision. As the sensitivity of GW instruments improves, we will be able to leverage the increased quantity and quality of the detected signals to test the no-hair theorem in richer and more accurate ways.

Acknowledgements

References

[1] M. Isi, M. Giesler, W. M. Farr, M. A. Scheel, and S. A. Teukolsky, *Testing the no-hair theorem with GW150914*, *Phys. Rev. Lett.* **123** (2019), no. 11 111102, [`arXiv:1905.00869`].

[2] C. V. Vishveshwara, *Stability of the schwarzschild metric*, *Phys. Rev. D* **1** (May, 1970) 2870–2879.

[3] W. H. Press, *Long Wave Trains of Gravitational Waves from a Vibrating Black Hole*, *Astrophys. J.* **170** (1971) L105–L108.

[4] S. A. Teukolsky, *Perturbations of a Rotating Black Hole. I. Fundamental Equations for Gravitational, Electromagnetic, and Neutrino-Field Perturbations*, ApJ **185** (Oct., 1973) 635–648.

[5] S. Chandrasekhar and S. Detweiler, *The quasi-normal modes of the schwarzschild black hole*, *Proc. R. Soc. A* **344** (1975), no. 1639 441–452.

[6] F. Echeverria, *Gravitational Wave Measurements of the Mass and Angular Momentum of a Black Hole*, *Phys. Rev.* **D40** (1989) 3194–3203.

[7] O. Dreyer, B. J. Kelly, B. Krishnan, L. S. Finn, D. Garrison, and R. Lopez-Aleman, *Black hole spectroscopy: Testing general relativity through gravitational wave observations*, *Class. Quant. Grav.* **21** (2004) 787–804, [`gr-qc/0309007`].

[8] E. Berti, V. Cardoso, and C. M. Will, *On gravitational-wave spectroscopy of massive black holes with the space interferometer LISA*, *Phys. Rev.* **D73** (2006) 064030, [`gr-qc/0512160`].

[9] S. Gossan, J. Veitch, and B. S. Sathyaprakash, *Bayesian model selection for testing the no-hair theorem with black hole ringdowns*, *Phys. Rev.* **D85** (2012) 124056, [`arXiv:1111.5819`].

[10] J. Meidam, M. Agathos, C. Van Den Broeck, J. Veitch, and B. S. Sathyaprakash, *Testing the no-hair theorem with black hole ringdowns using TIGER*, *Phys. Rev.* **D90** (2014), no. 6 064009, [`arXiv:1406.3201`].

[11] E. Berti et al., *Testing General Relativity with Present and Future Astrophysical Observations*, *Class. Quant. Grav.* **32** (2015) 243001, [`arXiv:1501.07274`].

[12] E. Berti, A. Sesana, E. Barausse, V. Cardoso, and K. Belczynski, *Spectroscopy of Kerr black holes with Earth- and space-based interferometers*, *Phys. Rev. Lett.* **117** (2016), no. 10 101102, [`arXiv:1605.09286`].

[13] V. Baibhav, E. Berti, V. Cardoso, and G. Khanna, *Black Hole Spectroscopy: Systematic Errors and Ringdown Energy Estimates*, *Phys. Rev.* **D97** (2018), no. 4 044048, [`arXiv:1710.02156`].

[14] V. Baibhav and E. Berti, *Multimode black hole spectroscopy*, *Phys. Rev.* **D99** (2019), no. 2 024005, [`arXiv:1809.03500`].

[15] J. Aasi et al., *Advanced LIGO*, *Class. Quant. Grav.* **32** (2015) 074001.

[16] **LIGO Scientific Collaboration, Virgo Collaboration** Collaboration, B. P. Abbott et al., *Observation of Gravitational Waves from a Binary Black Hole Merger*, *Phys. Rev. Lett.* **116** (feb, 2016) 061102.

[17] M. Giesler, M. Isi, M. A. Scheel, and S. Teukolsky, *Black Hole Ringdown: The Importance of Overtones*, *Phys. Rev. X* **9** (2019), no. 4 041060, [`arXiv:1903.08284`].

[18] **LIGO Scientific Collaboration, Virgo Collaboration** Collaboration, B. P. Abbott et al., *Tests of general relativity with GW150914*, *Phys. Rev. Lett.* **116** (2016) 221101, [`arXiv:1602.03841`].

[19] **LIGO Scientific Collaboration, Virgo Collaboration** Collaboration, B. P. Abbott et al., *Tests of General Relativity with GW150914*, *Phys. Rev. Lett.* **116** (may, 2016) 221101.

[20] W. Del Pozzo and A. Nagar, *Analytic family of post-merger template waveforms*, *Phys. Rev.* **D95** (2017), no. 12 124034, [`arXiv:1606.03952`].

[21] M. Cabero, C. D. Capano, O. Fischer-Birnholtz, B. Krishnan, A. B. Nielsen, A. H. Nitz, and C. M. Biwer, *Observational tests of the black hole area increase law*, *Phys. Rev.* **D97** (2018), no. 12 124069, [`arXiv:1711.09073`].

[22] E. Thrane, P. D. Lasky, and Y. Levin, *Challenges testing the no-hair theorem with gravitational waves*, *Phys. Rev.* **D96** (2017), no. 10 102004, [`arXiv:1706.05152`].

[23] R. Brito, A. Buonanno, and V. Raymond, *Black-hole Spectroscopy by Making Full Use of Gravitational-Wave Modeling*, *Phys. Rev.* **D98** (2018), no. 8 084038, [`arXiv:1805.00293`].

[24] G. Carullo et al., *Empirical tests of the black hole no-hair conjecture using gravitational-wave observations*, *Phys. Rev.* **D98** (2018), no. 10 104020, [`arXiv:1805.04760`].

[25] G. Carullo, W. Del Pozzo, and J. Veitch, *Observational Black Hole Spectroscopy: A time-domain multimode analysis of GW150914*, *Phys. Rev.* **D99** (2019), no. 12 123029, [`arXiv:1902.07527`].

[26] I. Kamaretsos, M. Hannam, S. Husa, and B. S. Sathyaprakash, *Black-hole hair loss: learning about binary progenitors from ringdown signals*, *Phys. Rev.* **D85** (2012) 024018, [`arXiv:1107.0854`].

[27] L. London, J. Healy, and D. Shoemaker, *Modeling Ringdown: Beyond the Fundamental Quasi-Normal Modes*, *Phys. Rev. D* **90** (2014) 124032, [`arXiv:1404.3197`].

[28] A. Buonanno, G. B. Cook, and F. Pretorius, *Inspiral, merger and ring-down of equal-mass black-hole binaries*, *Phys. Rev.* **D75** (2007) 124018, [`gr-qc/0610122`].

[29] Y. Pan, A. Buonanno, A. Taracchini, L. E. Kidder, A. H. Mroue, et al., *Inspiral-merger-ringdown waveforms of spinning, precessing black-hole binaries in the effective-one-body formalism*, *Phys. Rev. D* **89** (2013) 084006, [`arXiv:1307.6232`].

[30] A. Taracchini, A. Buonanno, Y. Pan, T. Hinderer, M. Boyle, D. A. Hemberger, L. E. Kidder, G. Lovelace, A. H. Mroue, H. P. Pfeiffer, M. A. Scheel, B. Szilagyi, N. W. Taylor, and A. Zenginoglu, *Effective-one-body model for black-hole binaries with generic mass ratios and spins*, *Phys. Rev. D* **89 (R)** (2014), no. 6 061502, [`arXiv:1311.2544`].

[31] S. Babak, A. Taracchini, and A. Buonanno, *Validating the effective-one-body model of spinning, precessing binary black holes against numerical relativity*, `arXiv:1607.05661`.

[32] S. Bhagwat, D. A. Brown, and S. W. Ballmer, *Spectroscopic analysis of stellar mass black-hole mergers in our local universe with ground-based gravitational wave detectors*, *Phys. Rev.* **D94** (2016), no. 8 084024, [`arXiv:1607.07845`]. [Erratum: Phys. Rev.D95,no.6,069906(2017)].

[33] Koudounia, "Church bell 6500gr."
https://koudounia.com/en/product/bells/church-bell/church-bell-3/.
Accessed: 2020-01-30.

[34] freepik, "Hammer closeup." https://www.freepik.com/premium-photo/
close-up-hand-holding-big-hammer-against-white-background_2744259.htm.
Accessed: 2020-01-30.

[35] **LIGO Scientific Collaboration, Virgo Collaboration** Collaboration, B. P. Abbott et al., *Directly comparing GW150914 with numerical solutions of Einstein's equations for binary black hole coalescence*, *Phys. Rev. D* **94** (2016) 064035, [arXiv:1606.01262].

[36] **LIGO Scientific Collaboration, Virgo Collaboration** Collaboration, B. P. Abbott et al., *Effects of waveform model systematics on the interpretation of GW150914*, *Class. Quant. Grav.* **34** (2017), no. 10 104002, [arXiv:1611.07531].

[37] E. W. Leaver, *An Analytic representation for the quasi normal modes of Kerr black holes*, *Proc. Roy. Soc. Lond.* **A402** (1985) 285–298.

[38] E. Berti, V. Cardoso, and A. O. Starinets, *TOPICAL REVIEW: Quasinormal modes of black holes and black branes*, *Class. Quantum Grav.* **26** (Aug., 2009) 163001, [arXiv:0905.2975].

[39] http://pages.jh.edu/~eberti2/ringdown.

[40] **LIGO Scientific, Virgo** Collaboration, B. P. Abbott et al., *GWTC-1: A Gravitational-Wave Transient Catalog of Compact Binary Mergers Observed by LIGO and Virgo during the First and Second Observing Runs*, arXiv:1811.12907.

[41] https://www.gw-openscience.org.

[42] **LIGO Scientific Collaboration, Virgo Collaboration** Collaboration, B. P. Abbott et al., *Properties of the Binary Black Hole Merger GW150914*, *Phys. Rev. Lett.* **116** (jun, 2016) 241102, [arXiv:1602.03840].

[43] V. Varma, D. Gerosa, L. C. Stein, F. Hebert, and H. Zhang, *High-accuracy mass, spin, and recoil predictions of generic black-hole merger remnants*, *Phys. Rev. Lett.* **122** (2019), no. 1 011101, [arXiv:1809.09125].

[44] J. Blackman, S. E. Field, M. A. Scheel, C. R. Galley, C. D. Ott, M. Boyle, L. E. Kidder, H. P. Pfeiffer, and B. Szilágyi, *Numerical relativity waveform surrogate model for generically precessing binary black hole mergers*, *Phys. Rev.* **D96** (2017), no. 2 024058, [arXiv:1705.07089].

[45] LIGO Scientific Collaboration and Virgo Collaboration, "GWTC-1."
https://doi.org/10.7935/82H3-HH23, 2018.

[46] A. Ghosh et al., *Testing general relativity using golden black-hole binaries*, *Phys. Rev. D* **94** (2016), no. 2 021101(R), [arXiv:1602.02453].

[47] A. Ghosh, N. K. Johnson-McDaniel, A. Ghosh, C. K. Mishra, P. Ajith, W. Del Pozzo, C. P. L. Berry, A. B. Nielsen, and L. London, *Testing general relativity using gravitational wave signals from the inspiral, merger and ringdown of binary black holes*, *Classical Quantum Gravity* **35** (2018), no. 1 014002, [arXiv:1704.06784].

[48] M. Vallisneri, J. Kanner, R. Williams, A. Weinstein, and B. Stephens, *The LIGO Open Science Center*, *J. Phys. Conf. Ser.* **610** (2015), no. 1 012021, [arXiv:1410.4839].